hPL-human adipose-derived stem cells in IKVAV-functionalised hydrogel conduit (Biogelx): an innovative delivery strategy to improve peripheral nerve repair

Dr Martino Guiotto (martino.guiotto4@gmail.com)
Department of Plastic, Reconstructive and Hand Surgery, Centre Hospitalier Universitaire Vaudois (CHUV), Lausanne, Switzerland

Dr Alison Clayton
Biogelx, Glasgow, United Kingdom

Dr Ryan Morgan
Biogelx, Glasgow, United Kingdom

Prof Wassim Raffoul
Department of Plastic, Reconstructive and Hand Surgery, Centre Hospitalier Universitaire Vaudois (CHUV), Lausanne, Switzerland

Prof Andrew Hart
Canniesburn Plastic Surgery Unit, Glasgow Royal Infirmary, Glasgow, United Kingdom

Dr Mathis Riehle
Centre for the Cellular Microenvironment, University of Glasgow, United Kingdom

Prof Pietro di Summa
Department of Plastic, Reconstructive and Hand Surgery, Centre Hospitalier Universitaire Vaudois (CHUV), Lausanne, Switzerland

Research Article

Keywords: Peripheral Nerve Injury, 15 mm Rat Sciatic Nerve, Human Adipose derived stem cells (ADSC), Human Platelet Lysate (hPL), IKVAV Biogelx, Cell Therapy, Peripheral Nerve Repair

Posted Date: July 28th, 2023

DOI: https://doi.org/10.21203/rs.3.rs-3210148/v1

Abstract

Background.

Adipose-derived stem cells (ADSC) are nowadays one of the most exploited cells in regenerative medicine. They are fast growing, capable of enhancing axonal elongation, support and locally stimulate Schwann cells (SC) and protect de-innervated muscles from atrophy after a peripheral nerve injury.

Methods.

With the aim of developing a bio-safe, clinically translatable cell-therapy, we assessed the effect of ADSC pre-expanded with human platelet lysate (hPL) in an *in vivo* rat model, delivering the cells into a 15 mm critical-size sciatic nerve defect embedded within a laminin-peptide-functionalised hydrogel (Biogelx-IKVAV) wrapped by a poly–caprolactone (PCL) nerve conduit.

Results.

ADSC retained their stemness, their immunophenotype and proliferative activity when tested *in vitro*. At six weeks post implantation, robust regeneration was observed across the critical-size gap as evaluated by both the axonal elongation (anti-NF 200) and SC proliferation (anti-S100) within the Biogelx-IKVAV filled PCL conduit. All the other experimental groups manifested significantly lower levels of growth cone elongation. The histological gastrocnemius muscle analysis was comparable with no quantitative significant differences among the experimental groups.

Conclusion.

Taken together, these results suggest that ADSC encapsulated in Biogelx-IKVAV are a potential path to improve the efficacy of nerve regeneration. New perspectives can be pursued for the development of a fully synthetic bioengineered nerve graft for the treatment of peripheral nerve injury.

Introduction

Injury to the peripheral nerve system (PNS) is a relatively common event in trauma care with devastating impact on quality of life. As young, working age patients are often affected, nerve injury leads to significant personal and socioeconomic costs. Autologous nerve graft remains the current gold standard in clinical practice when a tension-free direct suture between stumps is not possible. Despite the natural healing capacity of the PNS, the functional outcome is never fully satisfactory due to nerve cell death, with axons remaining disconnected and neuroma formation. Moreover, autografts may be associated with relevant morbidity of the nerve donor site areas. Successful treatment depends on the ability to promote greater numbers of axons reaching the distal stump and sustaining the intrinsic role of local Schwann cells (SC). (1, 2, 3, 4)

A wide range of strategies have been applied to *in vivo* models such as neural tubes, extra-cellular matrix (ECM)-functionalised nerve conduits, different types of support cells and growth factors (GF), often delivered by a variety of scaffolds. (2, 3, 5, 6)

Human adipose derived stem cells (hADSC) are an encouraging candidate for cell-based therapies in PNS repair, particularly when their properties are sustained and supported by a bio conduit.(1, 7, 8)

Based on previous research studies, we know that hADSC can be routinely isolated and cultured in a completely xenogeneic-free way by using human-platelet-lysate (hPL) supplemented culture medium, especially when in combination with collagenase digestion, without altering their physiology and stemness. (9, 10, 11)

The higher proliferation rate of hPL-expanded hADSC (hADSC-hPL), when compared with those grown with foetal bovine serum (FBS) supplemented medium, were associated with a statistically higher secretion of brain-derived neurotrophic factor (BDNF), glial cell-derived growth factor (GDNF) and nerve derived growth factor (NGF) than FBS-cultured cells, which in turn have been shown to increase neurite outgrowth in dorsal root ganglia (DRG)/hADSC co-cultures. (7, 9)

Guidance and support of the axonal regrowth through the nerve gap are the keys to achieve the optimal functional results; and ECM proteins guarantee structure and directionality in peripheral nerve regeneration (1, 3, 12, 13).

Based on our previous experiences on the interplay between hADSC-hPL (7, 9), hADSC-hPL grown on laminin (LN) can be a promising translatable path to sustain nerve regeneration, improving cell proliferation, supporting neurotropism while maintaining stable cell properties and bio safety profile. (7, 9, 14)

Self-assembling peptides (SAPs) can be used to create an advanced type of synthetic hydrogel capable of mimicking the native cell microenvironment, providing a tissue-like but completely synthetic ECM. The inherent control of the constituents makes these materials a promising option for biomedical tissue engineered applications, including neural conduit lumen-filling materials. (15, 16)

Synthetic peptides have several advantages compared to natural proteins, including ease of self-assembly, mechanical stability, excellent control of three-dimensional (3D) molecular structure, low immunogenic profile (17), which are based on the ability to fine-tune their physical, chemical, and mechanical properties. (18) Finally, peptide hydrogels can be tuned to have a porous structure that is useful for cell migration and nerve growth. (15) The encapsulation of hADSC in SAP hydrogels showed successful outcomes in a variety of different contexts; for instance, myocardial infarction (19) and bone regeneration. (20, 21)

In contrast to the well-established use of SAPs, the literature evidence is limited regarding ADSC integration in SAPs for a peripheral nerve repair scenario. (15)

Here, we investigated how a combinatorial approach using an injectable hydrogel (Biogelx) functionalised with a neuro-active, laminin-derived peptide (IKVAV) in combination with hADSC and a polymer containing conduit with topographic guidance, can influence nerve regeneration in an *in vivo* pre-clinical model.

Materials and Methods

hADSC extraction and culture

hADSC were isolated from abdominal adipose tissue of three healthy women (age 49 +/- 2) who underwent breast reconstruction using abdominal autologous flaps (Deep Inferior Epigastric Perforator flaps, DIEP) at Department of Plastic, Reconstructive and Hand Surgery, Centre Hospitalier Universitaire Vaudois (CHUV) in Lausanne. The discarded part of the flap and the adipose tissue were obtained after a signed informed consent. All protocols were reviewed and approved by the hospital ethic committee (Ethics State Committee regulations of the Department of Musculoskeletal Biobank (Lausanne)) in accordance with the Declaration of Helsinki.

The adipose tissue was mechanically minced, micro-dissected and tissue fragments (diameter: < 5mm) seeded in 10 cm Petri dishes. As hADSC adhere to and spread on tissue culture plastic, they self-select for continued culture.(22) Tissue fragments were suspended in 7ml of complete medium, plated in T75 flask and cultured at 37°C and 5% CO_2. The medium was changed after 24 hours to remove erythrocytes and afterwards every three or four days until cell confluence. Cells isolated were cultured in Alpha-MEM (Gibco, Paisley, UK) supplemented with 5% human Platelet Lysate (hPL, Antibodies, Aachen, Germany) and 1% Penicillin-Streptomycin (GE Healthcare).

HADSC immunophenotype and multi lineage differentiation potential were evaluated as previously described. (9) Briefly, hADSC lacked the expression of hematopoietic stem cells markers (< 2%, CD34 and CD45), while they were positive (> 90%) for CD105, CD73 and CD90. Moreover, hADSC differentiated into adipocytes and generated bone nodule like structures respectively, when exposed to the specific differentiation medium. Thus, mechanical dissociation followed by an hPL-supplemented expansion step does not affect the expression of stemness markers and maintains the hADSC multilineage differentiation potential, as previously showed by our group. (9)

Biogelx Preparation

The synthetic SAP hydrogels were obtained from Biogelx (Glasgow, UK). (23, 24) Two types of hydrogels were compared for the *in vitro* preliminary assessments (**S** – non functionalised and **IKVAV** – containing a LN-inspired neuro-interactive peptide. The target stiffness for the two gels was defined at $G' \approx 10$kPa at 1 Hz. The choice of a $G' \approx 10$kPa was based on sciatic nerve elastic properties according to previous rheological tests.(2) Gels were prepared according to the Biogelx guidelines (24).

In brief, a cell pellet (cell density, medium volume and time of incubation were defined according to the specific experiment, see below) was resuspended in the hydrogel powder mixed with sterile water (Pre-Gel Solution). After pipetting up and down to allow for a homogeneous cell distribution, the prepared pre-gel/cell solution was diluted in the required volume into the well plates.

Conditioning of the hydrogels was performed by mixing the cell/pre-gel mixtures with complete medium, followed by incubation of the plates at 37°C, 5% CO_2. Volumes and concentrations were defined following the Biogelx guidelines, according to the type of well plates and the experimental conditions.

Rheology

To determine mechanical properties of the gel before and following cell culture, hADSC (15000 cells/well in 96 well plates) were seeded in the hydrogel (3D culture) and rheological measurements were performed at days 3 and 7 for both the gel types (S and IKVAV). Cell cultures in the gel matrix were fixed in 4% PFA for 15 minutes at 37°C then washed and kept in PBS 1% until the rheological analysis. Measurements were performed in parallel on gels kept in tissue culture conditions without cells as controls. All rheological studies were undertaken using a stress-controlled rotational rheometer Kinexus 2100 series. Frequency sweeps were carried out from 0.1 Hz to 100 Hz, at constant oscillation amplitude and temperature, and with a working gap of 0.5 mm. From the graph of storage modulus against frequency produced, the stiffness of the sample was calculated. The geometry of the circular reader was PU8 (8 mm diameter).

hADSC cell viability and proliferation assay

Live and dead cell viability assay was performed after 48 hours of hADSC 3D (cell density 750000/ml in 24 well plates) culture in Biogelx S and IKVAV according to the manufacturer protocol (Thermofisher Scientific, USA).

The cell viability and proliferation were monitored on days 3 and 7 using Alamar Blue (AB) assay according to the manufacturer protocol (Sigma Aldrich, USA). Briefly, 10% AB solution was added to each sample, including negative controls and incubated at 37°C, 5% CO_2 for 4 h. Supernatant of the reacted solution was transferred into a 96-well plate and the absorbance was read at 570 and 600 nm with a plate reader. The proliferative potential related to the metabolic activity was then expressed as the percentage reduction of the AB reagent, calculated as follows:

$$\%Reduced\ (Cell\ Viability) = \frac{((\varepsilon_{ox\_600} \times A_{570}) - (\varepsilon_{ox\_570} \times A_{600}))}{((\varepsilon_{red\_570} \times C_{600}) - (\varepsilon_{red\_600} \times C_{570}))} \times 100$$

A_{570} and A_{600} are the absorbance values of each sample at 570 and 600 nm respectively, C_{570} and C_{600} the absorbance values of the negative controls; $\varepsilon_{ox\_600} = 117.216$, $\varepsilon_{ox\_570} = 80.586$, $\varepsilon_{red\_600} = 14.652$ and $\varepsilon_{red\_570} = 155.677$ the molar extinction coefficients of the AB reagent in the oxidized and reduced form.

Poly-ℰ-caprolactone conduit preparation

Poly-ℰ-caprolactone (PCL, Sigma-Aldrich, UK 440744, MW 80000) was dissolved in chloroform (Fisher Scientific, UK) at 12% wt./vol. and mixed on the shaker for at least 48 hours to provide a homogenous solution. The resultant mixture (3 ml/78.6cm^2) was spin-coated (SPIN 150 Master) for 30 seconds (1000 RPM, 100 RPM/s acceleration) onto a 10 cm PDMS master bearing topographical cues, grooves, pillars, pits. The resultant 20µm thin film was dried off with filtered (0.2µm) compressed air for 10 minutes.

The PCL membrane was rolled around a sterile needle G14 (conduit inner diameter of 1.8 mm) and thermally sealed by the application of the edge of the metallic slide heated to 80°C. Finally, the tube obtained was cut into conduits of the desired length (17 mm).

Based on previous experience at CeMi, a lateral overlap (after rolling) of the polymer sheet of 3.5 mm provides a good seal without compromising internal structure, integrity and flexibility (4, 25). Conduit length and diameter were verified under microscopic magnification to assess reproducibility of the technique before implantation.

Experimental animals

All animal protocols were approved by the local veterinary commission in canton Vaud (Lausanne), Switzerland and were carried out in accordance with the 3R standard care for animal experimentation. Male Wistar rats (Janvier, France) weighing 200 g were used for this study.

Experimental design and surgical procedure

Seven experimental groups were included: PCL conduit without cells (Empty), PCL conduit seeded with hADSC (hADSC), PCL conduit with Biogelx-S encapsulating hADSC (hADSC-S), PCL conduit with Biogelx-IKVAV encapsulating hADSC (hADSC-IKVAV), PCL conduit with Biogelx-S (S), PCL conduit with Biogelx-IKVAV (IKVAV) and a control group composed of autograft (Autograft). The statistical power and sample size were defined (G*Power, version 3.1) according to our previous experience (effect size between 2 and 3, Beta error = 0.8, alpha error = 0.05) and considering an average autotomy rate for Lewis male rats

around 10%. We increased the minimum number of rats for each group to 6 subjects (total number 42). (26)

Two to 4 hours before implantation, cells were trypsinized and after centrifugation, $1x10^6$ cells suspended in 50–70 µL of serum free growth medium (99% Alpha-MEM and 1% Pen-Strep) and these encapsulated into the SAP gel (3D culture following the Biogelx protocols for *in vitro* cell cultures as previously described) or seeded in the PCL conduit (in the first hour of incubation, the conduit was rotated by 90° every 20 minutes in order to facilitate the equal distribution/seeding of the hADSC on the entire inner surface of the conduit.

After having induced deep anesthesia with isoflurane (Attane™, Piramal Enterprises Ltd.), the operation was performed on the left sciatic nerve under aseptic conditions using a power focus surgical microscope (Carl Zeiss, Germany). A skin incision from the left knee to the hip was made for exposure of the underlying muscles, which were then retracted to reveal the sciatic nerve. The sciatic nerve was transected and both nerve stumps were fixed to the conduit by a single epineural “telescopic” suture (9/0 Prolene, Ethicon, Germany): proximal and distal nerve ends were inserted 1 mm into the tube, thus leaving a 15 mm gap. In the autograft group, after dissection of the sciatic nerve, a 15 mm segment was excised, reversed and sutured on each side by two epineural sutures. Muscles and fascia layers were closed with single resorbable stitches (4/0 Monocryl, Ethicon, Germany) and the skin by a single points suture (4/0 Prolene, Ethicon, Germany). All experimental groups were housed on sawdust, two animals per cage with a 12 h light:12 h dark cycle (lights on at 06.00 h) and received food and water *ad libitum*. (Fig. 1)

Nerve conduit harvesting and immunohistochemistry

Six weeks after surgery, the animals were euthanized with an intra peritoneal injection of sodium pentobarbital and decapitation. The regenerated left sciatic nerves were harvested under operating microscope together with proximal and distal stumps.

Harvested conduits were fixed with 4% PFA over night at RT, then immersed in PBS containing 15% sucrose for 4–6 hours, then 30% sucrose overnight at RT. The following day, specimens were embedded in OCT freezing media (Tissue-tek, Sakura, Japan), and frozen at -80°C for at least 3 days. Longitudinal cryo-sections (12 µm) were prepared and immediately placed onto slides.

After a fixation (PFA 4%) and re-hydration step (5 min in sterile water), a permeabilization solution 0.25% Triton X-100 in PBS for 10 mins at RT was applied followed by 1% bovine serum albumin (BSA)/phosphate buffered saline (PBS) blocking and incubation of the slides overnight with primary antibodies anti-NF200 (1:500, rabbit, Abcam ab207176) or anti-S100 (1:500, rabbit, Abcam ab34686). The following day after 3–5 min PBS Tween 0.025% washing step, slides were incubated with secondary antibody (1:500, Alexa Fluor goat anti-rabbit, Abcam ab 150077) at room temperature in the dark for 1 hour. After a further 3–5 min PBS Tween 0.025% washing step, the slides were finally mounted with Vectashield with DAPI (Vector Labs, UK) and examined under the fluorescence microscope (10x magnification) with the regenerating conus directed towards the distal end. Axonal regeneration distance

(NF200) and S100 positive cell distribution inside the conduit were evaluated using a Nanozoomer slide scanner (Hamamatsu) and NDP view 2.0 software (Hamamatsu). The length of NF200 and S100 was measured using the beginning of the conduit as a starting point to the end, which was defined by the last clearly visible sprout of the regenerating conus.

Histomorphometry analyses of the gastrocnemius muscle

Using an operating microscope (Leica Microsystems), both left and right (control) gastrocnemius muscles were carefully cleaned and dissected out, dividing their tendinous origin and insertion from the bone. The gastrocnemius muscle (lateral bundle) was immobilized in formalin, dehydrated in graded alcohol, and embedded in paraffin, sections (3 µm) were cut perpendicular to the length, through the largest part of the muscle belly and stained with Masson's Trichrome using standard methods, and then observed under a light microscope (Axioscan, Leica Microsystems).

Histomorphometry was performed (10x magnification) to quantify the number of muscle fibers and the cross-sectional area of muscle fibers within the gastrocnemius muscle. At the same time measurements for the contralateral muscle were obtained in order to have a representative value, independently of the size of the animal and variation in growth pattern between animals (ratio).

Statistical analysis

All measurements of the *in vitro* investigation were repeated three times technically to ensure reproducibility with three different patient cell sources.

All data were expressed as average ± standard error (SE) of the mean.

One-way analysis of variance (ANOVA) with Tukey's multiple comparison test was used to assess statistical significance among three or more groups. Significance was expressed as *$p < 0.05$, **$p < 0.01$, ***$p < 0.001$, $p < 0.0001$ ****. All analysis was performed using GraphPad Prism 6 for Mac (GraphPad Software, La Jolla California USA).

Results

Biogelx is a suitable scaffold for hPL-hADSC

Prior to *in vivo* application, the SAP scaffold was tested *in vitro*, particularly focusing on cell viability in the Biogelx system. A cytotoxicity assay after 48 hours showed that more than 80% of cells were alive within the SAP substrates without any significant difference between the two types of gels (S or IKVAV). AB assay was applied to investigate the viability/proliferation of hADSC in Biogelx with both 2D and 3D cultures.

Regarding the proliferation assay, cell metabolic activity detected by AB reduction was assessed between 30–40% when cells were placed in 3D cultures after 3 and 7 days. (Fig. 2)

When hADSC were seeded on top of hydrogel (2D), the AB assay detected values between 45–70% (Fig. 3).

In both 2D and 3D cultures, no significant differences were observed between the two types of hydrogels tested in the same timeline. (Figs. 2 and 3)

However, the IKVAV-gel seemed to enable good proliferation, particularly when ADSC were seeded on top of the SAP gel. Indeed, in 2D, the reductive activity was significantly different between day 3 and 7 only for the IKVAV type ($p < 0.01$ **, Fig. 3), while the S type did not seem to increase the cell proliferation in a time-dependent manner (no significant difference between day 3 and 7). Interestingly, in the 3D system, cell proliferation was significantly higher in both types of gel ($p < 0.001$ ****), between the 3rd and 7th days (Fig. 2).

hPL-hADSC influence the mechanical properties of Biogelx hydrogels over time

The rheological measurement of G' and G" of the hydrogels (n = 3) showed that they were mechanically stable between 0.1 and 100 Hz and that elastic properties (G', dark lines, Fig. 4A **and B**) dominate their behaviour. We observed a reduction in elastic and viscoelastic properties in the cell filled gels over time, starting evidently to take effect between days 3and 7. This significant (S type $p < 0.001$ ***, IKVAV type $p < 0.01$ ** between day 3 and 7) reduction in G' and G" may indicate a cell-based rearrangement or partial degradation of the hydrogel. Optically, the gels did not change and were just as easy to manipulate.

In vivo surgeries and macroscopic outcomes

39 animals survived, 1 rat died before surgery due to isoflurane overdosage, 2 rats were sacrificed at postoperative day 2 and 3 respectively because of an open wound (criteria for euthanasia in our study). The dissection of the conduits at the end of the experiment revealed no kinking of the nerve tube and revealed a repair site that was intact with no gross abnormalities or evidence of ongoing healing. No autotomy was reported during the entire six weeks experiment.

Axonal Regeneration-immunohistochemistry

Sciatic nerve axonal regeneration was evaluated by measuring the distance that NF200 positive axons were able to cover from the proximal stump; to reveal and assess SC infiltration, slides were stained for S100 (Fig. 5) as previously reported (27). The axons crossing the conduits filled with hADSC encapsulated within Biogelx IKVAV (12.1 ± 0.85 mm) covered significantly longer distances compared to: empty conduits (3.6 ± 1.4 mm, $p < 0.0001$ ****); conduits filled with the hydrogels (S: 6.7 ± 0.69 mm, $p < 0.0001$ **** or IKVAV: 7.4 ± 1.92 mm, $p < 0.001$ ***); and conduits filled only with hADSC (8.4 ± 0.85 mm, $p < 0.01$ *) (Fig. 6).

When cell-free Biogelx filled conduits were applied, axonal regeneration was significantly longer than those in an empty conduit (S $p < 0.05$ *, IKVAV $p < 0.01$ **). Conduits seeded with hADSC resulted in

meaningful nerve regeneration compared with empty conduit treatment ($p < 0.001$ ***), but did not show any significant difference when compared to cell-free Biogelx filled (Fig. 6).

The distances over which S100 positive cells migrated from the stumps into the conduit showed a similar pattern to that seen for NF200: empty conduit showed some ingrowths (3.9 ± 2.04 mm), whereas filling the conduits with Biogelx IKVAV (8.17 ± 1.99 mm) significantly increased the migration distance of SC ($p < 0.05$ *). ADSC filled conduits resulted in a similar growing path as adding IKVAV hydrogel (9.22 ± 0.93 mm). Finally, hADSC encapsulated in Biogelx IKVAV (11.96 ± 1.90 mm) obtained the highest meaningful growth profile ($p < 0.001$ **** VS empty, $p < 0.05$ * VS IKVAV). (Fig. 6).

Histomorphometry of gastrocnemius muscle

The gastrocnemius muscle (GM) was analysed for changes to evaluate eventual different levels of muscular atrophy after sciatic transection and repair. Masson's Trichrome staining was used to evaluate the morphology of GM fibers in cross-sections taken at the maximal transversal belly diameter, evaluating the effects that each experimental treatment had on muscle structure. After six weeks, from a qualitative perspective, the experimental conditions evidenced a smaller muscle fiber cross sectional area and a higher number of nuclei/area compared to the contralateral (sciatic nerve not transected) control without any significant differences in terms of quantitative analysis between the experimental groups, the autograft and controls (data not shown) (Fig. 7).

Discussion

Cell therapy is a promising treatment to approach peripheral nerve injuries, as demonstrated by a vast number of pre-clinical *in vitro* and *in vivo* research studies. (28, 29, 30) For autologous cell therapy, ADSC have been identified as ideally suited, as they are abundant, easily expandable and have been shown to have positive effects on nerve regeneration. (31, 32, 33, 34)

Although cell-therapy is a valuable approach, significant concerns remain around cell survival following transplantation *in vivo*, the persistence and the duration of ADSC neurotropic properties/effects in the recipient neural microenvironment. (10, 35, 36) One of the open questions is the delivery method in an *in vivo* scenario, which permits cell survival; and supports and exploits the properties of the transplanted cells longer term. In fact, direct cell injection into the injury site has shown poor engraftment outcomes: ADSC injected at the nerve gap has only had a survival rate of about 0.5% and are undetectable 2 weeks after their application. (36, 37, 38) Multiple hypotheses have been advanced, such as the intense local inflammatory response after nerve transection, mechanical damage endured during injection, (39) or the high concentration of adenosine triphosphate that has been shown to induce cell death via P27X receptors in ADSC and Schwann cells after peripheral nerve injury. (37, 40)

For all these reasons, a wide range of biomaterial carriers have been tested, with the aim to maintain therapeutic cells in a suitable state for sufficient time to permit exploitation of their beneficial effects. Recently, research efforts are being focused on developing a bio-engineered scaffold modified with ECM

proteins, or their bioactive moieties, with adjusted viscoelastic properties and tailored degradation profiles, to optimize cell retention and functional maintenance at the injury site. (3, 41, 42, 43, 44, 45, 46)

The introduction of ECM molecules provides an enriched environment for cell adhesion and migration, activating and/or inhibiting cell signalling pathways that in turn can act on regenerative and survival biochemical factors. (47, 48, 49) Specifically, LN was selected in developing an engineered nerve construct, due to its critical role in myelin formation and axonal sorting (50), with similar findings obtained using laminin-derived peptide sequences, particularly RGD and IKVAV. (51)

Short peptide molecules were shown to self-assemble into water-swollen networks forming highly biocompatible and biodegradable SAP hydrogels with ideal properties for biomedical applications. (52, 53) The SAP hydrogels used here, and synthesized by Biogelx, consist of interwoven nanofibers of ca. 10 nm in diameter with pore sizes ranging between ca. 10 and 200 nm which provide a suitable 3D environment for cell growth and allow the diffusion of small soluble factors. The Biogelx scaffold fibers and pores are smaller than the cells' diameter and similar to the dimensions seen in the native ECM thus, cells can adhere to the microfibers. While they are somewhat embedded in the nanofibrous scaffold, they are free to move and interact with each other and their environment. (15, 52, 54, 55)

Previous studies demonstrated that functionalised SAP hydrogels promoted cell attachment, proliferation and migration of multiple cell types including osteoblasts (56), human umbilical vein endothelial cells, hADSC and SC. (57, 58)

Considering the development of ADSC-therapy strategy for peripheral nerve repair, we chose one of the LN-derived peptides, the IKVAV, which was affirmed earlier as a supportive factor of neuronal growth cone adhesion and elongation (50). As shown in our previous studies with LN, and widely confirmed by the literature, IKVAV also contributes to the support of ADSC viability, proliferation and neurotrophic cell commitment. (5, 7, 9) Our ADSC viability assessment confirmed the significant enhanced proliferation in Biogelx-IKVAV between the 3rd and 7th day compared to the S type gel, particularly in a 2D system.

Consistently, previous studies found that YIGSR (another LN-peptide) and RGD mediated SC adhesion and proliferation, while IKVAV drove neural differentiation and enhanced nerve regeneration by supporting the axonal elongation both *in vitro* and *in vivo*. (59) Santiago et al. found that the hADSC adhere preferentially to the IKVAV peptidescompared to two other LN-derived peptide counterparts RGD and YIGSR. (60)

Moreover, recent studies investigated the combination of LN or LN peptide (IKVAV) and growth factors (e.g., BDNF) for nerve repair: Park et al. fabricated a hyaluronic acid-based hydrogel with the IKVAV peptide and full length BDNF molecule incorporated into a 3D scaffold for the treatment of spinal cord injury. The introduction of this conduit resulted in faster differentiation of stem cells and facilitated nerve regeneration. (61) Then, Frick et al. developed an injectable IKVAV-functionalised SAP hydrogel, which incorporates BDNF, promoting attachment and favourable neurite outgrowth of spiral ganglion neurons in

cochlear implants. (62) Again, LN-binding BDNF was widely applied in pre-clinical models, for the treatment of cerebral ischemia, facial nerve injury and recurrent laryngeal nerve injury. (63, 64, 65)

Therefore, using the ADSC expanded in hPL and encapsulated in Biogelx IKVAV, we combined the synergetic effects of ADSC-therapy, the ECM and the hPL growth factor enrichment (14) with a 3D SAP support. Biogelx-based laminin scaffold could be a simplified method that overcomes the drawbacks of current delivery systems, stimulating the transplanted cells through peptide functionalization, adaptable stiffness and guaranteeing biosafety during clinical translation.

In this work, such hybrid cell–gel systems, loaded into microfabricated PCL conduits to support regeneration, were tested initially *in vitro* in terms of cell viability and proliferation, then *in vivo* over a period of six weeks, in terms of peripheral nerve sprouting and gastrocnemius muscle histology.

The axonal regeneration through the 15 mm sciatic nerve defect was evaluated by the distances reached by regenerating axons and SC in longitudinal sections of the explanted conduits. Scaffolds filled with hADSC encapsulated into Biogelx-IKVAV (hADSC-IKVAV) achieved significantly higher values both in terms of longest axonal sprouting and furthest SC migration along the regenerative growth cone compared to the empty conduit (empty, $p < 0.0001$ ****), the ones filled with hydrogel only (S, IKVAV, $p < 0.001$ ***) or cells only (hADSC, $p < 0.01$ **). Moreover, cells alone or hydrogel only achieved significantly higher axonal length than the empty conduit (S $p < 0.05$ *, IKVAV $p < 0.01$ **), but only IKVAV gained a similar significant trend in SC migration distance ($p < 0.05$ *). However, no significant differences, both in terms of axonal elongation and SC migration distance were found between cells alone and gels only: these results underline how the effects of hADSC are dependent on an adequate delivery/support system and how the polyvalent value of IKVAV can impact both ADSC and neural cells.

Overall, these effects could be most likely ascribed to the complementary roles of hADSC-IKVAV to assure cell-to-cell interactions with regrowing axons, release and maintenance of the hADSC secretome (e.g., growth factors such as NGF, vascular endothelial growth factor, and BDNF) with its slow progressive release in the local milieu (31, 66). Each of these molecules is essential for the recruitment of endogenous SC at the site of a peripheral nerve injury, improving tissue regeneration and functional repair. Furthermore, the functionalization with LN-derived IKVAV-peptide can further enhance survival and neurotrophic properties of transplanted hADSC and directly stimulate axonal regrowth.(5, 7)

Regarding the histological muscle analysis, no quantitative significant differences were found among the experimental groups, as could probably be expected after a 15mm critical sciatic nerve gap and only 6 weeks experiment. Indeed, although axonal regrowth through the nerve gap was observed, the muscle changes at the level of muscle fiber composition take place over a longer time period than six weeks, as other studies have shown (67). The trend of a higher ratio nuclei/muscle fiber area could be explained by a denser infiltration of inflammatory cells or a more intense recruitment of satellite cells around the muscle fibers, particularly in the experimental conditions (IKVAV, hADSC) with an additive effect between the cells and hydrogel components (hADSC-IKVAV). Both inflammatory cell and satellite cell tissue

invasion/recruitment are initial signs of muscle regeneration, but again, the earlier timeline considered here cannot be significantly diriment in supporting our hypothesis. (68, 69, 70)

A longer-term study (12 weeks) will also be critical to evaluate potential muscle recovery after denervation, together with behavioural, functional, and histological outcomes.

Conclusion

Overall, our findings show that Biogelx-IKVAV scaffold has innovative potential applicability as a delivery vehicle for ADSC in peripheral nerve injury by allowing cell adhesion, cell growth, and maintenance of their neurotrophic properties, as well as axonal outgrowth. hADSC encapsulated into Biogelx functionalised with IKVAV combines easy applicability together with an advanced tissue engineering solution, aiming towards future clinical translation in peripheral nerve repair.

Abbreviations List

Brain-derived neurotrophic factor (BDNF)

Cluster of differentiation (CD)

Dorsal root ganglia (DRG)

Extra-Cellular matrix (ECM)

Foetal bovine serum (FBS)

Gastrocnemius muscle (GM)

Glial cell-derived growth factor (GDNF)

Good manufacturing practice (GMP)

Growth factors (GFs)

Human adipose derived stem cells (hADSC)

Human platelet lysate (hPL)

Mesenchymal stem cells (MSCs)

Nerve derived growth factor (NGF)

Peripheral nerve injuries (PNI)

Peripheral nerve system (PNS)

Poly–caprolactone (PCL)

Self-assembling peptides (SAPs)

Schwann cells (SCs)

Declarations

Ethics approval and consent to participate

All protocols regarding human samples (in Lausanne) were reviewed and approved by the hospital (Centre Hospitalier Universitaire Vaudois CHUV)) according to Ethics State Committee regulations of the Department of Musculoskeletal Biobank (Lausanne) in accordance with the Declaration of Helsinki. Adipose tissue collection is under Protocol #12/2012 “Department of Musculoskeletal Medicine Biobank conservation of biological human material for research and use” following all of the rules and regulations of this program approved by the State Ethics Board.

All animal work was carried out in accordance with the Animal License Cantonal Number VD3630 (National number 33070, application title *“HPL-human adipose-derived stem cells into a smart functionalized hydrogel conduit (BiogelX-IKVAV) in peripheral nerve repair: an in vivo assessment with a critical rat sciatic nerve defect model”*, approved 19.03.2021 (for the period 2021-2024)) for the care and use of laboratory animals approved by local veterinary commission in Canton Vaud, Switzerland.

Consent for publication

Not Applicable

Availability of data and materials

The datasets used and/or analysed during the current study are available from the corresponding author on reasonable request and deposited at the University of Lausanne.

Competing interests

The authors declare that they have no competing interests

Funding

Leenaards Fondation financially supported this research project.

Authors' contributions

MG did the experiments, analysed the data and wrote the manuscript. MG and PGdS conceived the idea. PGdS with MOR supervised the project and corrected the manuscript. AC and RM did the hydrogel

rheological measurements. All the authors (MG, PGdS, MOR, AMH, WR, AC and RM) read, critically revised, and approved the final version of the manuscript.

Acknowledgements

We are grateful to the *Leenaards Fondation* for granting this project.

We thank Prof. Applegate for welcoming the first author at the Regenerative Cell Therapy lab at UNIL-CHUV, and all her staff for technical support and precious insights. The authors are grateful to the Yannick Krempp and his collaborators of the CIF (University of Lausanne) for the extremely useful suggestions in images capturing and analysis. Finally, we want to acknowledge Dr. Tedeschi (University of Bari) for kindly translate into a graphic illustration the abstract.

References

1. di Summa PG, Kalbermatten DF, Pralong E, Raffoul W, Kingham PJ, Terenghi G. Long-term in vivo regeneration of peripheral nerves through bioengineered nerve grafts. Neuroscience. 2011;181:278-91.
2. Faroni A, Workman VL, Saiani A, Reid AJ. Self-Assembling Peptide Hydrogel Matrices Improve the Neurotrophic Potential of Human Adipose-Derived Stem Cells. Adv Healthc Mater. 2019;8(17):e1900410.
3. de Luca AC, Lacour SP, Raffoul W, di Summa PG. Extracellular matrix components in peripheral nerve repair: how to affect neural cellular response and nerve regeneration? Neural Regen Res. 2014;9(22):1943-8.
4. E. TS. Translational development of a three-dimensional bioactive conduit for peripheral nerve repair, through the application of topographical cues and stem cell support. 2017.
5. di Summa PG, Kalbermatten DF, Raffoul W, Terenghi G, Kingham PJ. Extracellular matrix molecules enhance the neurotrophic effect of Schwann cell-like differentiated adipose-derived stem cells and increase cell survival under stress conditions. Tissue Eng Part A. 2013;19(3-4):368-79.
6. Xu Z, Orkwis JA, DeVine BM, Harris GM. Extracellular matrix cues modulate Schwann cell morphology, proliferation, and protein expression. J Tissue Eng Regen Med. 2019.
7. Guiotto M, Raffoul W, Hart AM, Riehle MO, di Summa PG. Human Platelet Lysate Acts Synergistically With Laminin to Improve the Neurotrophic Effect of Human Adipose-Derived Stem Cells on Primary Neurons. Front Bioeng Biotechnol. 2021;9:658176.
8. Di Summa PG, Schiraldi L, Cherubino M, Oranges CM, Kalbermatten DF, Raffoul W, et al. Adipose Derived Stem Cells Reduce Fibrosis and Promote Nerve Regeneration in Rats. Anat Rec (Hoboken). 2018;301(10):1714-21.
9. Palombella S, Guiotto M, Higgins GC, Applegate LL, Raffoul W, Cherubino M, et al. Human platelet lysate as a potential clinical-translatable supplement to support the neurotrophic properties of human adipose-derived stem cells. Stem Cell Res Ther. 2020;11(1):432.

10. Guiotto M, Raffoul W, Hart AM, Riehle MO, di Summa PG. Human platelet lysate to substitute fetal bovine serum in hMSC expansion for translational applications: a systematic review. J Transl Med. 2020;18(1):351.
11. Guiotto M, Riehle MO, Raffoul W, Hart A, di Summa PG. Is human platelet lysate (hPL) the ideal candidate to substitute the foetal bovine serum for cell-therapy translational research? J Transl Med. 2021;19(1):426.
12. Modrak M, Talukder MAH, Gurgenashvili K, Noble M, Elfar JC. Peripheral nerve injury and myelination: Potential therapeutic strategies. J Neurosci Res. 2020;98(5):780-95.
13. di Summa PG, Kingham PJ, Raffoul W, Wiberg M, Terenghi G, Kalbermatten DF. Adipose-derived stem cells enhance peripheral nerve regeneration. J Plast Reconstr Aesthet Surg. 2010;63(9):1544-52.
14. di Summa PG, Madduri S. Synergy of human platelet lysate and laminin to enhance the neurotrophic effect of human adipose-derived stem cells. Neural Regen Res. 2022;17(10):2200-2.
15. Yang S, Wang C, Zhu J, Lu C, Li H, Chen F, et al. Self-assembling peptide hydrogels functionalized with LN- and BDNF- mimicking epitopes synergistically enhance peripheral nerve regeneration. Theranostics. 2020;10(18):8227-49.
16. Alakpa EV, Jayawarna V, Burgess KEV, West CC, Péault B, Ulijn RV, et al. Improving cartilage phenotype from differentiated pericytes in tunable peptide hydrogels. Sci Rep. 2017;7(1):6895.
17. Markey A, Workman VL, Bruce IA, Woolford TJ, Derby B, Miller AF, et al. Peptide hydrogel in vitro non-inflammatory potential. J Pept Sci. 2017;23(2):148-54.
18. Gu Y, Zhu J, Xue C, Li Z, Ding F, Yang Y, et al. Chitosan/silk fibroin-based, Schwann cell-derived extracellular matrix-modified scaffolds for bridging rat sciatic nerve gaps. Biomaterials. 2014;35(7):2253-63.
19. Kim JH, Park Y, Jung Y, Kim SH. Combinatorial therapy with three-dimensionally cultured adipose-derived stromal cells and self-assembling peptides to enhance angiogenesis and preserve cardiac function in infarcted hearts. J Tissue Eng Regen Med. 2017;11(10):2816-27.
20. Haastert-Talini K, Geuna S, Dahlin LB, Meyer C, Stenberg L, Freier T, et al. Chitosan tubes of varying degrees of acetylation for bridging peripheral nerve defects. Biomaterials. 2013;34(38):9886-904.
21. Yang H, Hong N, Liu H, Wang J, Li Y, Wu S. Differentiated adipose-derived stem cell cocultures for bone regeneration in RADA16-I in vitro. J Cell Physiol. 2018;233(12):9458-72.
22. Maxence KhhS, Anthony G, Murielle M, Wassim R, A AL. Enhancement of Human Adipose-Derived Stem Cell Expansion and Stability for Clinical use. Int J Stem Cell Res Ther2015.
23. Jayawarna V, Richardson SM, Hirst AR, Hodson NW, Saiani A, Gough JE, et al. Introducing chemical functionality in Fmoc-peptide gels for cell culture. Acta Biomater. 2009;5(3):934-43.
24. Alakpa EV JV, Lampel A, Burgess KV, West CC, Bakker SCJ, Roy S, Javid N, Fleming S, Lamprou DA, Yang JL, Miller A, Urquhart AJ, Frederix PWJM, Hunt NT, Peault B, Ulijn RV, Dalby MJ. Tunable Supramolecular Hydrogels for Selection of Lineage-Guiding Metabolites in Stem Cell Cultures2016.

25. Thomson SE, Charalambous C, Smith CA, Tsimbouri PM, Déjardin T, Kingham PJ, et al. Microtopographical cues promote peripheral nerve regeneration via transient mTORC2 activation. Acta Biomater. 2017;60:220-31.
26. Faul F, Erdfelder E, Buchner A, Lang AG. Statistical power analyses using G*Power 3.1: tests for correlation and regression analyses. Behav Res Methods. 2009;41(4):1149-60.
27. Madduri S, di Summa P, Papaloïzos M, Kalbermatten D, Gander B. Effect of controlled co-delivery of synergistic neurotrophic factors on early nerve regeneration in rats. Biomaterials. 2010;31(32):8402-9.
28. Faroni A, Smith RJ, Reid AJ. Adipose derived stem cells and nerve regeneration. Neural Regen Res. 2014;9(14):1341-6.
29. Faroni A, Mobasseri SA, Kingham PJ, Reid AJ. Peripheral nerve regeneration: experimental strategies and future perspectives. Adv Drug Deliv Rev. 2015;82-83:160-7.
30. Tohill M, Terenghi G. Stem-cell plasticity and therapy for injuries of the peripheral nervous system. Biotechnol Appl Biochem. 2004;40(Pt 1):17-24.
31. Kingham PJ, Kolar MK, Novikova LN, Novikov LN, Wiberg M. Stimulating the neurotrophic and angiogenic properties of human adipose-derived stem cells enhances nerve repair. Stem Cells Dev. 2014;23(7):741-54.
32. Reid AJ, Sun M, Wiberg M, Downes S, Terenghi G, Kingham PJ. Nerve repair with adipose-derived stem cells protects dorsal root ganglia neurons from apoptosis. Neuroscience. 2011;199:515-22.
33. Tomita K, Madura T, Sakai Y, Yano K, Terenghi G, Hosokawa K. Glial differentiation of human adipose-derived stem cells: implications for cell-based transplantation therapy. Neuroscience. 2013;236:55-65.
34. Tomita K, Madura T, Mantovani C, Terenghi G. Differentiated adipose-derived stem cells promote myelination and enhance functional recovery in a rat model of chronic denervation. J Neurosci Res. 2012;90(7):1392-402.
35. Lindroos B, Suuronen R, Miettinen S. The potential of adipose stem cells in regenerative medicine. Stem Cell Rev Rep. 2011;7(2):269-91.
36. Walsh SK, Kumar R, Grochmal JK, Kemp SW, Forden J, Midha R. Fate of stem cell transplants in peripheral nerves. Stem Cell Res. 2012;8(2):226-38.
37. Faroni A, Rothwell SW, Grolla AA, Terenghi G, Magnaghi V, Verkhratsky A. Differentiation of adipose-derived stem cells into Schwann cell phenotype induces expression of P2X receptors that control cell death. Cell Death Dis. 2013;4:e743.
38. Erba P, Mantovani C, Kalbermatten DF, Pierer G, Terenghi G, Kingham PJ. Regeneration potential and survival of transplanted undifferentiated adipose tissue-derived stem cells in peripheral nerve conduits. J Plast Reconstr Aesthet Surg. 2010;63(12):e811-7.
39. Foster AA, Marquardt LM, Heilshorn SC. The Diverse Roles of Hydrogel Mechanics in Injectable Stem Cell Transplantation. Curr Opin Chem Eng. 2017;15:15-23.

40. Luo J, Lee S, Wu D, Yeh J, Ellamushi H, Wheeler AP, et al. P2X7 purinoceptors contribute to the death of Schwann cells transplanted into the spinal cord. Cell Death Dis. 2013;4:e829.
41. Jiang L, Jones S, Jia X. Stem Cell Transplantation for Peripheral Nerve Regeneration: Current Options and Opportunities. Int J Mol Sci. 2017;18(1).
42. Kohn-Polster C, Bhatnagar D, Woloszyn DJ, Richtmyer M, Starke A, Springwald AH, et al. Dual-Component Gelatinous Peptide/Reactive Oligomer Formulations as Conduit Material and Luminal Filler for Peripheral Nerve Regeneration. Int J Mol Sci. 2017;18(5).
43. Gattazzo F, Urciuolo A, Bonaldo P. Extracellular matrix: a dynamic microenvironment for stem cell niche. Biochim Biophys Acta. 2014;1840(8):2506-19.
44. de Luca AC, Faroni A, Downes S, Terenghi G. Differentiated adipose-derived stem cells act synergistically with RGD-modified surfaces to improve neurite outgrowth in a co-culture model. J Tissue Eng Regen Med. 2016;10(8):647-55.
45. Rao F, Wang Y, Zhang D, Lu C, Cao Z, Sui J, et al. Aligned chitosan nanofiber hydrogel grafted with peptides mimicking bioactive brain-derived neurotrophic factor and vascular endothelial growth factor repair long-distance sciatic nerve defects in rats. Theranostics. 2020;10(4):1590-603.
46. Du J, Liu J, Yao S, Mao H, Peng J, Sun X, et al. Prompt peripheral nerve regeneration induced by a hierarchically aligned fibrin nanofiber hydrogel. Acta Biomater. 2017;55:296-309.
47. Chernousov MA, Stahl RC, Carey DJ. Schwann cell type V collagen inhibits axonal outgrowth and promotes Schwann cell migration via distinct adhesive activities of the collagen and noncollagen domains. J Neurosci. 2001;21(16):6125-35.
48. Chernousov MA, Yu WM, Chen ZL, Carey DJ, Strickland S. Regulation of Schwann cell function by the extracellular matrix. Glia. 2008;56(14):1498-507.
49. Rao SS, Winter JO. Adhesion molecule-modified biomaterials for neural tissue engineering. Front Neuroeng. 2009;2:6.
50. Tashiro K, Sephel GC, Weeks B, Sasaki M, Martin GR, Kleinman HK, et al. A synthetic peptide containing the IKVAV sequence from the A chain of laminin mediates cell attachment, migration, and neurite outgrowth. J Biol Chem. 1989;264(27):16174-82.
51. Hosseinkhani H, Hiraoka Y, Li CH, Chen YR, Yu DS, Hong PD, et al. Engineering three-dimensional collagen-IKVAV matrix to mimic neural microenvironment. ACS Chem Neurosci. 2013;4(8):1229-35.
52. Gao J, Tang C, Elsawy MA, Smith AM, Miller AF, Saiani A. Controlling Self-Assembling Peptide Hydrogel Properties through Network Topology. Biomacromolecules. 2017;18(3):826-34.
53. Caliari SR, Burdick JA. A practical guide to hydrogels for cell culture. Nat Methods. 2016;13(5):405-14.
54. Ulijn RV, Smith AM. Designing peptide based nanomaterials. Chem Soc Rev. 2008;37(4):664-75.
55. Yan C, Pochan DJ. Rheological properties of peptide-based hydrogels for biomedical and other applications. Chem Soc Rev. 2010;39(9):3528-40.

56. Horii A, Wang X, Gelain F, Zhang S. Biological designer self-assembling peptide nanofiber scaffolds significantly enhance osteoblast proliferation, differentiation and 3-D migration. PLoS One. 2007;2(2):e190.
57. Liu X, Wang X, Ren H, He J, Qiao L, Cui FZ. Functionalized self-assembling peptide nanofiber hydrogels mimic stem cell niche to control human adipose stem cell behavior in vitro. Acta Biomater. 2013;9(6):6798-805.
58. Lu C, Wang Y, Yang S, Wang C, Sun X, Lu J, et al. Bioactive Self-Assembling Peptide Hydrogels Functionalized with Brain-Derived Neurotrophic Factor and Nerve Growth Factor Mimicking Peptides Synergistically Promote Peripheral Nerve Regeneration. ACS Biomater Sci Eng. 2018;4(8):2994-3005.
59. Motta CMM, Endres KJ, Wesdemiotis C, Willits RK, Becker ML. Enhancing Schwann cell migration using concentration gradients of laminin-derived peptides. Biomaterials. 2019;218:119335.
60. Santiago LY, Nowak RW, Peter Rubin J, Marra KG. Peptide-surface modification of poly(caprolactone) with laminin-derived sequences for adipose-derived stem cell applications. Biomaterials. 2006;27(15):2962-9.
61. Park J, Lim E, Back S, Na H, Park Y, Sun K. Nerve regeneration following spinal cord injury using matrix metalloproteinase-sensitive, hyaluronic acid-based biomimetic hydrogel scaffold containing brain-derived neurotrophic factor. J Biomed Mater Res A. 2010;93(3):1091-9.
62. Frick C, Müller M, Wank U, Tropitzsch A, Kramer B, Senn P, et al. Biofunctionalized peptide-based hydrogels provide permissive scaffolds to attract neurite outgrowth from spiral ganglion neurons. Colloids Surf B Biointerfaces. 2017;149:105-14.
63. Wang B, Yuan J, Xu J, Chen X, Ying X, Dong P. Brain-derived and glial cell line-derived neurotrophic factor fusion protein immobilization to laminin. Exp Ther Med. 2017;13(1):178-86.
64. Han Q, Li B, Feng H, Xiao Z, Chen B, Zhao Y, et al. The promotion of cerebral ischemia recovery in rats by laminin-binding BDNF. Biomaterials. 2011;32(22):5077-85.
65. Wang B, Yuan J, Chen X, Xu J, Li Y, Dong P. Functional regeneration of the transected recurrent laryngeal nerve using a collagen scaffold loaded with laminin and laminin-binding BDNF and GDNF. Sci Rep. 2016;6:32292.
66. Mahay D, Terenghi G, Shawcross SG. Growth factors in mesenchymal stem cells following glial-cell differentiation. Biotechnol Appl Biochem. 2008;51(Pt 4):167-76.
67. Jonsson S, Wiberg R, McGrath AM, Novikov LN, Wiberg M, Novikova LN, et al. Effect of delayed peripheral nerve repair on nerve regeneration, Schwann cell function and target muscle recovery. PLoS One. 2013;8(2):e56484.
68. Schmidt M, Schüler SC, Hüttner SS, von Eyss B, von Maltzahn J. Adult stem cells at work: regenerating skeletal muscle. Cell Mol Life Sci. 2019;76(13):2559-70.
69. Passipieri JA, Dienes J, Frank J, Glazier J, Portell A, Venkatesh KP, et al. Adipose Stem Cells Enhance Nerve Regeneration and Muscle Function in a Peroneal Nerve Ablation Model. Tissue Eng Part A. 2021;27(5-6):297-310.

70. Karalaki M, Fili S, Philippou A, Koutsilieris M. Muscle regeneration: cellular and molecular events. In Vivo. 2009;23(5):779-96.

Figures

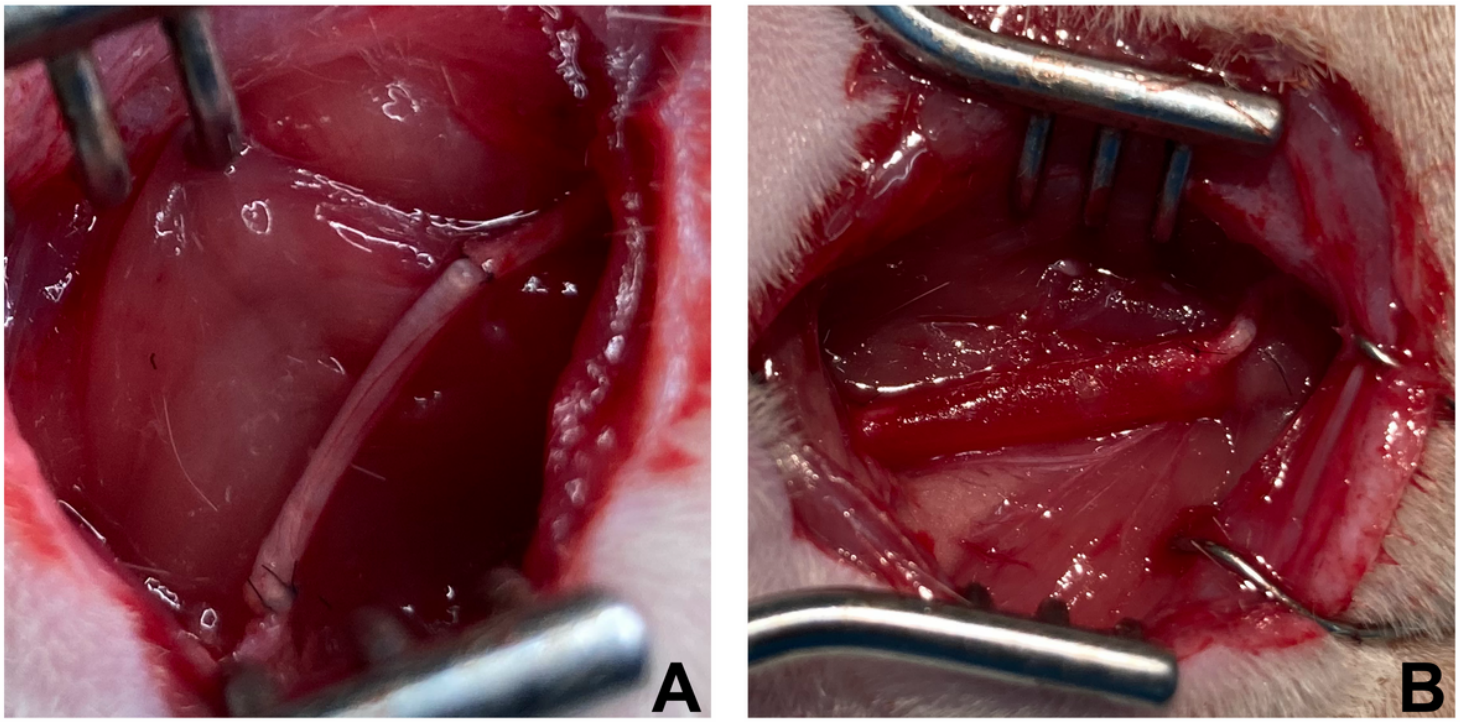

Figure 1

Surgical access on in vivo rat model. Autograft (A) and PCL nerve conduit filled with encapsulated hADSC into Biogelx-IKVAV (B) implanted in a 15 mm sciatic nerve gap.

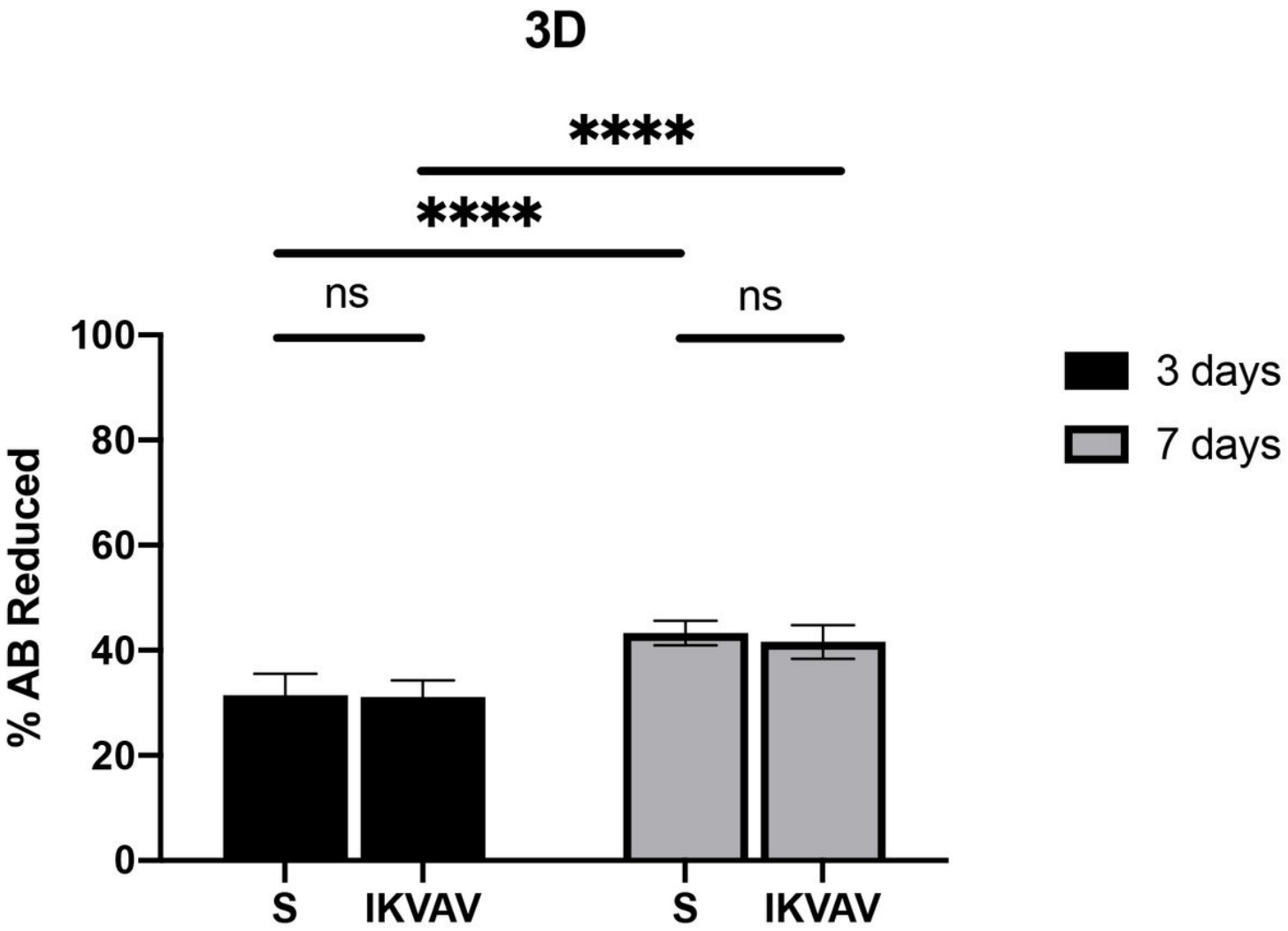

Figure 2

Proliferation Assay (Alamar Blue) of hADSC encapsulated in (3D) Biogelx at 3 and 7 days. S: Biogelx without peptide-functionalisation, IKVAV: Biogelx laminin-derived peptide-functionalised.

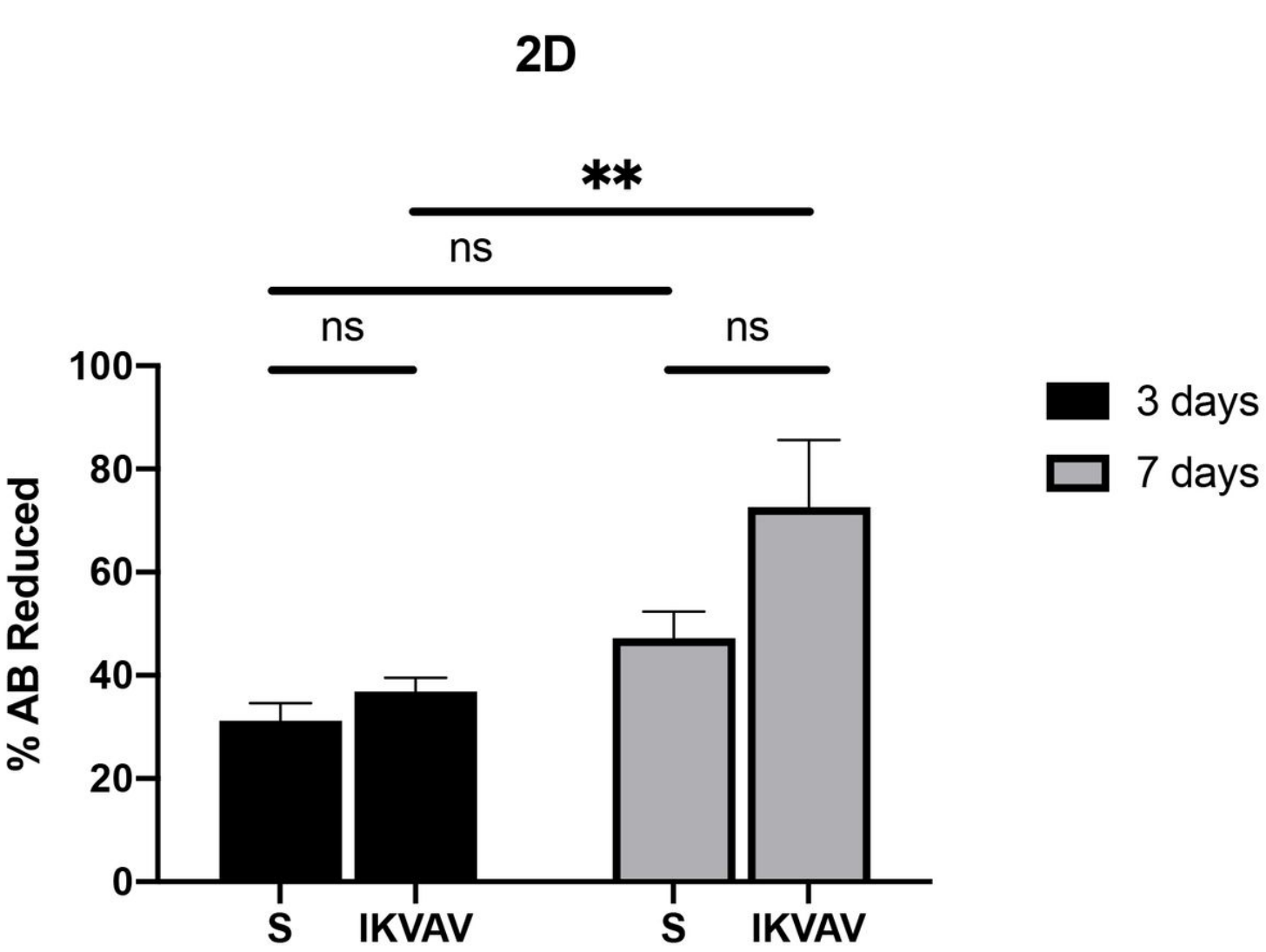

Figure 3

Proliferation Assay (Alamar Blue) of hADSC on top (2D) of Biogelx at 3 and 7 days. S: Biogelx without peptide-functionalisation, IKVAV: Biogelx laminin-derived peptide-functionalised.

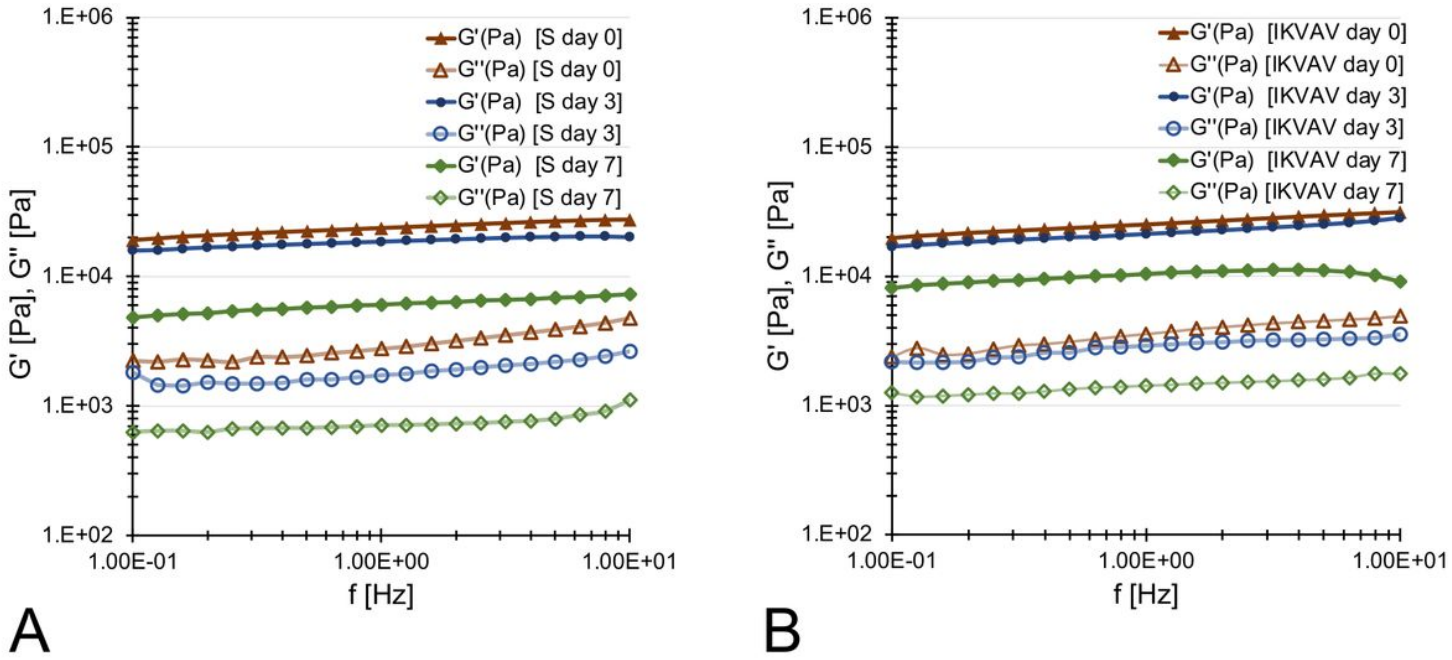

Figure 4

A and B. Rheology of empty and hADSC loaded Biogelx gels over seven days. Exemplary data for a frequency sweep of 0.1-100 Hz on days 0 (empty, triangles, brown), 3 days (hADSC loaded, circles, blue) and 7 days (hADSC loaded, diamonds, green), with G' shown in a dark, filled markers and G" in lighter colour outlined markers. 4A) Rheology of hADSC loaded S type, unmodified Biogelx gels over seven days. 4B) Rheology of hADSC loaded IKVAV modified Biogelx gels over seven days.

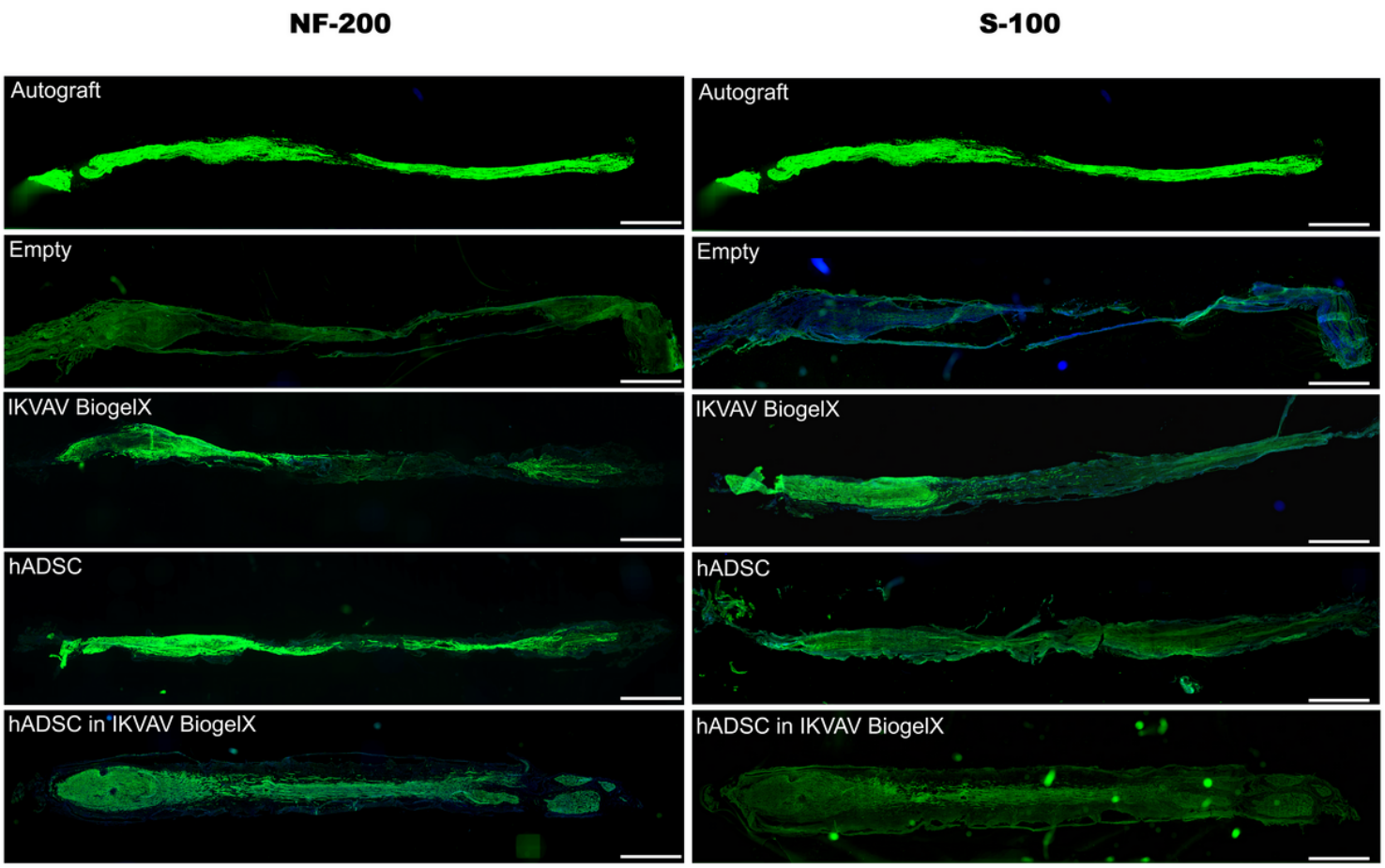

Figure 5

NF-200 staining (left side) shows axonal regeneration in different experimental conditions: autograft, empty conduit or filled with Biogelx IKVAV or seeded with hADSC or filled with encapsulated hADSC into Biogelx IKVAV. S-100 staining (right side) shows the proximal Schwann cell migration in different experimental conditions: autograft, empty conduit or filled with Biogelx IKVAV or seeded with hADSC or filled with encapsulated hADSC into Biogelx IKVAV. Nanozoomer 10x. NDP View 2 Software. Scale bar 1.5 mm

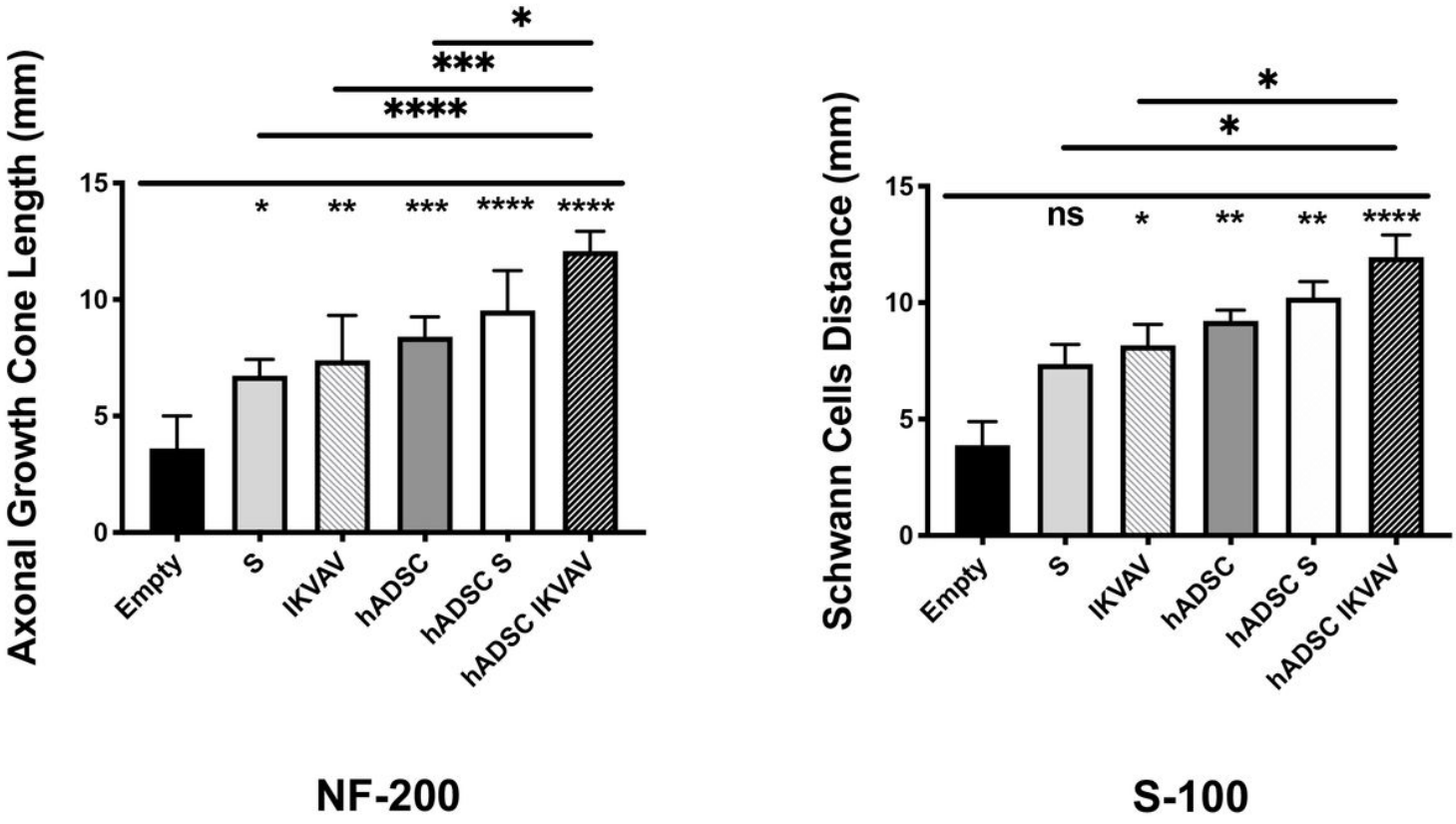

Figure 6

Quantitative evaluation of axonal growth cone fibers length (NF-200, left graph bar) and Schwann cells migration distance (S-100, right graph bar) in the same growth cone for all the experimental conditions: empty conduit, conduit filled with Biogelx S type or IKVAV type, conduit seeded with hADSC, conduit filled with encapsulated hADSC into Biogelx S type or IKVAV type. Values are mean distances (mm) ±SEM. (*p<0.05; **p<0.01; ***p<0.001, ****p<0.0001).

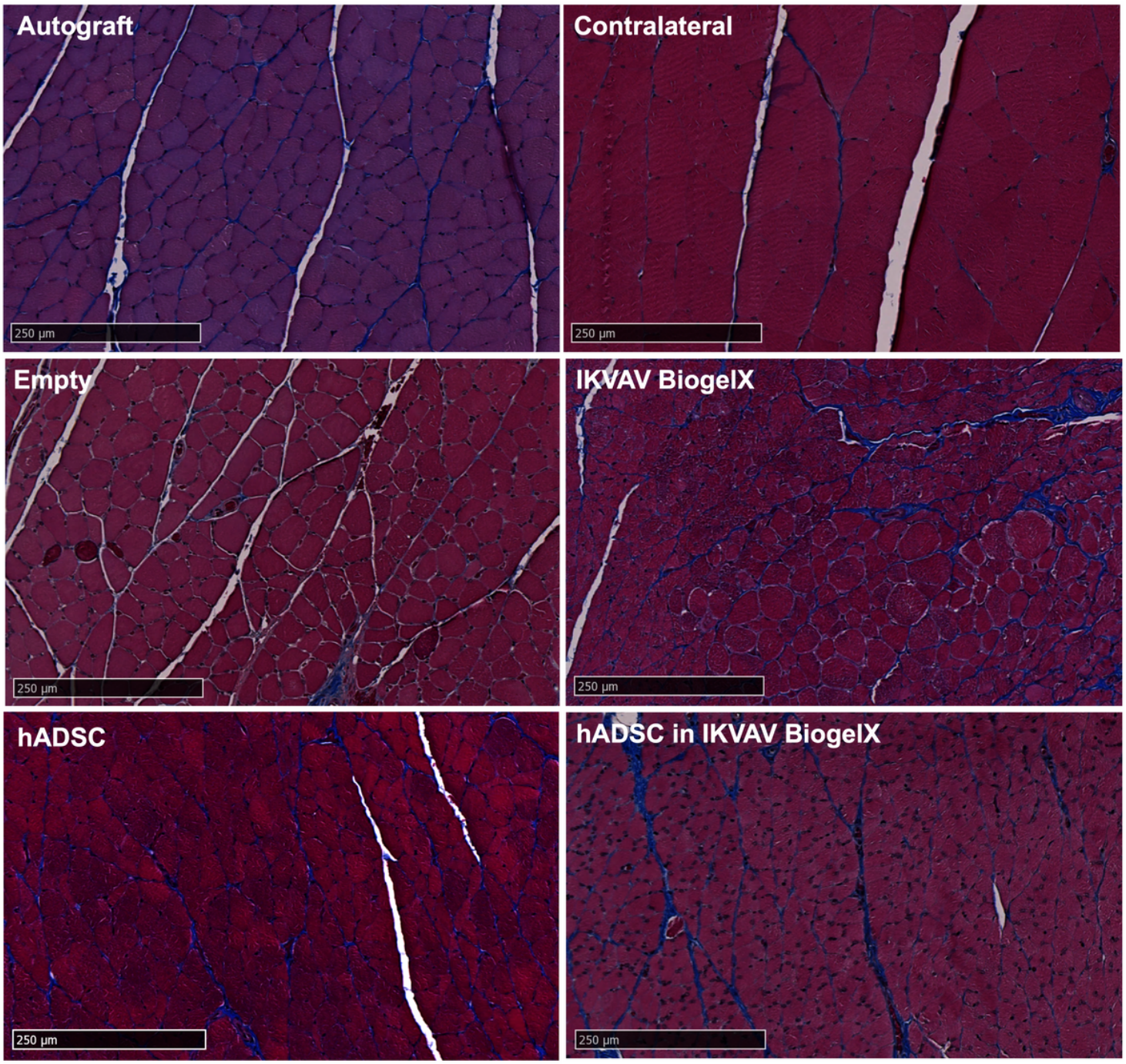

Figure 7

Qualitative assessment of muscle fibers adaptation after total sciatic nerve transection in all the experimental conditions (Autograft, Empty, Biogelx-IKVAV, hADSC, hADSC in Biogelx-IKVAV) and negative control (no transected nerve group – contralateral GM). Axioscan 10x. NDP View 2 Software. Scale bar 250 µm.

Supplementary Files

This is a list of supplementary files associated with this preprint. Click to download.

- GraphicalAbstract.jpg